Proceedings of the Korean Nuclear Society Spring Meeting
Pohang, Korea, May 1999

Application of H_∞ Control Theory to PWR Power Control

Sung Goo Chi [1] and Nam Zin Cho

Korea Advanced Institute of Science and Technology
Department of Nuclear Engineering
373-1 Kusong-dong, Yusong-gu
Taejon, Korea 305-701

Abstract

In this paper, a robust controller is designed by the use of H_∞ control theory for the PWR power control. The design specification is incorporated by the frequency weights using the mixed-sensitivity problem. The robustness of H_∞ control is verified by comparing with the classical output feedback control and LQG control in the case of measurement delay of the power measurement system. The H_∞ optimal control shows excellent stability-robustness and performance-robustness for external disturbances and noises, model parameter variations, and modeling errors. It also provides a practical design method because the design specification can be easily implemented.

I. Introduction

A major difficulty in implementing an optimal control theory such as Linear Quadratic Gaussian (LGG) is the lack of robustness. The model used to formulate the optimal control law cannot exactly match the physical process dynamics. The discrepancy between the actual process and its model can arise from modeling errors, model parameter variations, and external disturbances and noises. The controller should be designed so that the system dynamic performance-robustness and stability-robustness are met. A control system has performance-robustness when the controller has the capabilities of command follow, disturbance rejection, and insensitivity to sensor noise as well as the accommodation of hardware failure.

The H_∞ optimal filter was applied to estimate the reactivity using the linear and nonlinear point kinetics model [1,2]. The H_∞ control theory was applied to solve the reactivity instability problem in BWR power control and for PWR power control without the mixed sensitivity problem [3,4]. In this paper, a robust controller is designed by the use of H_∞ control theory for the PWR power control. The design specification is incorporated by the frequency weights using the mixed-sensitivity problem. The

---

* Present Address : Korea Power Engineering Company, Inc.

robustness of H_∞ control is verified by comparing with the classical output feedback control and LQG control in the case of measurement delay of the power measurement system.

II. Reactor Model

The nominal PWR model for controller design used in this paper is point kinetics with one delayed neutron group and temperature feedback from lumped fuel and coolant temperatures [5,6,7]. The reactor model with classical output feedback control is shown in Figure 1. The point kinetics equations with one delayed neutron group are as follows:

$$\frac{dn}{dt} = \frac{\delta\rho - \beta}{l} n + \lambda c, \tag{1}$$

$$\frac{dc}{dt} = \frac{\beta}{l} n - \lambda c, \tag{2}$$

The differential equation formulations for the lumped fuel and coolant temperatures are as follows :

$$W_f C_f \frac{dT_f}{dt} = f_f P_o(t) - UL(T_f - T_c), \tag{3}$$

$$W_c C_c \frac{dT_{out}}{dt} = (1 - f_f) P_o(t) + UL(T_f - T_c) - MC(T_{out} - T_{in}). \tag{4}$$

The reactivity input and feedback to point kinetics equations are represented by

$$\frac{d\delta\rho_r}{dt} = G_r z_r, \tag{5}$$

$$\delta\rho = \delta\rho_r + \alpha_f (T_f - T_{f0}) + \alpha_c (T_c - T_{c0}), \tag{6}$$

where $\delta\rho_r$ is the reactivity due to the control rod, G_r is the reactivity worth of the rod per unit length, and z_r is the control rod speed.

The simple first-order lag model is applied to model the dynamics of the power measurement system. The transfer function is given as follows :

$$G_n(s) = \frac{k_n}{\tau_n s + 1}. \tag{7}$$

After normalizing and linearizing the above equations around an equilibrium point, the following state-space representation is obtained as :

$$\frac{dx}{dt} = Ax + Bu, \quad y = Cx. \tag{8}$$

The state x and control u vectors are defined as $x = [\delta n_r \; \delta c_r \; \delta T_f \; \delta T_{out} \; \delta\rho_r \; \delta x_n]^T$ and $u = [z_r]$, respectively. A, B, C matrices in the state-space representation are

$$A=\begin{bmatrix} -\frac{\beta}{l} & \frac{\beta}{l} & \frac{n_{ro}\sigma_f}{l} & \frac{n_{ro}\sigma_c}{2l} & \frac{n_{ro}}{l} & 0 \\ \lambda & -\lambda & 0 & 0 & 0 & 0 \\ \frac{f_f P_{oo}}{W_f C_f} & 0 & -\frac{UL}{W_f C_f} & \frac{UL}{2W_f C_f} & 0 & 0 \\ \frac{(1-f_f)P_{oo}}{W_c C_c} & 0 & \frac{UL}{W_c C_c} & -\frac{(2MC+UL)}{2W_c C_c} & 0 & 0 \\ 0 & 0 & 0 & 0 & 0 & 0 \\ \frac{1}{\tau_n} & 0 & 0 & 0 & 0 & -\frac{1}{\tau_n} \end{bmatrix}, B=\begin{bmatrix} 0 \\ 0 \\ 0 \\ 0 \\ G_r \\ 0 \end{bmatrix}, \quad (9)$$

$C=[0\ 0\ 0\ 0\ 0\ 1]$.

III. H_∞ Optimal Control

The standard setup of H_∞ optimal control is shown in Figure 2. In this figure, w, u, z, and y are the exogenous input (consisting of command signals, disturbances, and sensor noises), the control signals, the output to be controlled, and the measured output, respectively. The transfer matrices P(s) and K(s) represent a generalized plant and a controller, respectively. Then, Figure 2 stands for the following algebraic equations by partitioning P(s) :

$$\begin{aligned} z &= P_{11}w + P_{12}u, \\ y &= P_{21}w + P_{22}u, \\ u &= Ky, \end{aligned} \quad (10)$$

with a state-space realization of the generalized plant P given by

$$P(s)=\begin{bmatrix} A & B_1 & B_2 \\ C_1 & D_{11} & D_{12} \\ C_2 & D_{21} & D_{22} \end{bmatrix}. \quad (11)$$

The transfer matrix from w to z is a linear-fractional transformation of K(s) as follows:

$$T_{zw} = P_{11} + P_{12}K(I - P_{22})^{-1}P_{21}. \quad (12)$$

The control objective of the standard H_∞ control problem is to find a rational-real proper K(s) to minimize the H_∞ norm of $T_{zw}(s)$ under the constraint that K(s) stabilizes P(s).

According to the general H_∞ algorithm [8,9], for the general control configuration of Figure 2 with valid assumptions, there exists a stabilized controller K(s) such that $\| T_{zw} \|_\infty < \gamma$ if and only if :

1) $X_\infty \geq 0$ is a solution to the Algebraic Riccati Equation (ARE)

$$A^T X_\infty + X_\infty A + C_1^T C_1 + X_\infty(\gamma^{-2}B_1B_1^T - B_2B_2^T)X_\infty = 0 \quad (13)$$

such that $Re\ \lambda_i[A + (\gamma^{-2}B_1B_1^T - B_2B_2^T)X_\infty] < 0, \forall i$; and

2) $Y_\infty \geq 0$ is a solution to the ARE

$$AY_\infty + Y_\infty A^T + B_1^T B_1 + Y_\infty(\gamma^{-2}C_1^T C_1 - C_2^T C_2)Y_\infty = 0 \quad (14)$$

such that $Re\ \lambda_i[A + Y_\infty(\gamma^{-2}C_1^T C_1 - C_2^T C_2)] < 0, \forall i$; and

3) $\rho(X_\infty Y_\infty) < \gamma^2$, where $\rho(A)$ is the spectral radius of A. (15)

Then, the controller is given by $K(s) = -Z_\infty L_\infty (sI - A_\infty)^{-1} F_\infty$,

where $F_\infty = -B_2^T X_\infty$, $L_\infty = -Y_\infty C_2^T$, $Z_\infty = (I - \gamma^{-2} Y_\infty X_\infty)^{-1}$, (16)

$A_\infty = A + \gamma^{-2} B_1 B_1^T X_\infty + B_2 F_\infty + Z_\infty L_\infty C_2$.

The controller can be separated into a state estimator and a state feedback as follows :

$$\frac{d\hat{x}}{dt} = A\hat{x} + B_1\gamma^{-2}B_1^T X_\infty \hat{x} + B_2 u + Z_\infty L_\infty (C_2\hat{x} - y), \quad u = F_\infty \hat{x} \ . \tag{17}$$

Figure 2 shows the model based controller consisting of the state estimator and state feedback.

The closed-loop response is expressed as follows :

$$y = Tr + SG_d d - Tn \tag{18}$$

where r = reference input, d = disturbance, n = noise, G_d = disturbance model

$L = PK$: loop transfer function

$S(s) = (1 + PK)^{-1} = (1 + L)^{-1}$: sensitivity function

$T(s) = 1 - S(s) = (1 + PK)^{-1} PK = (1 + L)^{-1} L$: complementary sensitivity function

The Bode plot of each of S(s) and T(s) plays an important role in the robust control system design. The Bode plot of S(s) determines the disturbance attenuation since S(s) is the closed-loop transfer function from disturbance to plant output error. The Bode plot of T(s) is used to measure the stability margin of the feedback system in the face of the multiplicative plant perturbations. Hence, it is desirable to make both of these two function as small as possible.

The disturbance rejection specification can be written as :

$$|S(s)| < \frac{1}{|W_S|} \Leftrightarrow \| W_S S \|_\infty < 1 \tag{19}$$

where $|W_S(s)|$ is the desired disturbance rejection frequency weight. Considering addition of a disturbance with low frequency, $|W_S(s)|$ is assigned to large values in the low-frequency range.

The robustness stability specification can be written as :

$$|T(s)| < \frac{1}{|W_T|} \Leftrightarrow \| W_T T \|_\infty < 1 \tag{20}$$

where $|W_T(s)|$ is the size of the largest anticipated multiplicative plant disturbance. Considering the plant disturbance to be in the high-frequency range, $|W_T(s)|$ is assigned to large values in the high-frequency range. The disturbance rejection specification and robust stability specification can be combined into a single norm of the form as :

$$\left\| \begin{matrix} W_S S \\ W_T T \end{matrix} \right\|_\infty < 1 \tag{21}$$

The problem of obtaining K(s) to satisfy Eq.(21) is called the mixed sensitivity problem. The control objective of the mixed sensitivity problem is to find a stabilized controller

K(s) such that the closed-loop transfer function $T_{zw}(s)$ is internally stable and its H_∞ norm is < 1.

IV. Simulation Results

Figures 4 and 5 show classical output feedback control reactor response for the step change in relative power demand from 100% to 110% without and with measurement delay, respectively. The value of τ_d is assumed to be 0.1 and 1.0 in Figures 4 and 5, respectively. Figures 6 and 7 show LQG control reactor response for 10% power step change without and with measurement delay, respectively. The solution of the LQG problem is known as the Separation Theorem [8,9]. It consists of first determining the optimal control to a deterministic linear quadratic regulator (LQR) problem. The optimal state estimate is given by a Kalman filter. In the LQG control, the design specification is incorporated by trial-error method. Even after the design specification is determined, the LQG based controller could show poor performance when the uncertainty is added to the plant model.

Figure 8 shows the frequency characteristics of the sensitivity S(s) and complementary sensitivity T(s) with the weights $|W_S(s)|$ and $|W_T(s)|$. The frequency weight $|W_S(s)|$ was selected to make the sensitivity S(s) satisfying the performance specification. The frequency weight $|W_T(s)|$ was selected to make the complementary sensitivity satisfying the robust specification. In this paper, the following frequency weights were selected to meet the desired specifications :

$$\text{Case 1 : } W_S(s)=\frac{1}{s+0.0025},\quad W_T(s)=\frac{0.1s^2+s}{325} \tag{22}$$

$$\text{Case 2 : } W_S(s)=\frac{1}{s+0.0025},\quad W_T(s)=\frac{0.1s^2+s}{5}$$

Figures 9 through 12 show the H_∞ control reactor response for 10% step change without and with measurement delay with Case 1 and Case 2 frequency weights, respectively. As shown in these figures, the time responses were not changed in the face of the hardware failure such as measurement delay under the assumption of no constraint of the control input (i.e., rod speed). Time response depends on the frequency weight, which is determined by design specifications.

V. Summary and Conclusions

The H_∞ optimal control shows excellent stability-robustness and performance-robustness for external disturbances and noises, model parameter variations, and modeling errors. It also provides a practical design method because the design specification can be easily implemented. For more realistic simulation, the nonlinear plant model should be used. To control the axial power distribution and the reactor power

simultaneously (i.e., load follow operation), the xenon and iodine equations should be considered in designing H_∞ controller.

References

1. K. Suzuki, et. al., "Estimation of Time-Varying Reactivity by the H_∞ Optimal Linear Filter," Nucl. Sci. Eng., 119, 128 (1995).
2. K. Suzuki, et. al., "Estimation of Dynamic Reactivity Using an H_∞ Optimal Filter with a Nonlinear Term," Nucl. Tech., 113, 145 (1995).
3. K. Suzuki, et. al., "Application of H_∞ Control Theory to Power Control of a Nonlinear Reactor Model," Nucl. Sci. Eng., 115, 142 (1993).
4. Y. J. Lee and J. I. Choi, "Robust Controller Design for the Nuclear Reactor Power Control System," J. Korean Nuc. Soci., 29, 280-290, (1996).
5. R. M. Edward, et. al., "State Feedback Assisted Classical Control : An Incremental Approach to Control Modernization of Existing and Future Nuclear Reactors and Power Plants," Nucl. Tech., 92, 167 (1990).
6. R. M. Edward, et. al., "Robust Optimal Control of Nuclear Reactors and Power Plants," Nucl. Tech., 98, 137 (1992).
7. R. M. Edward, et. al., "LQG/LTR Robust Control of Nuclear Reactors with Improved Temperature Performance," IEEE Tran. Nucl. Sci., 39, 2286 (1992).
8. K. Zbou, Robust and Optimal Control, Prentice-Hall, Inc., (1996).
9. S. Skogestad and I. Postlethwaite, Multivariable Feedback Control Analysis and Design, John Wiley & Sons., Inc., (1997).

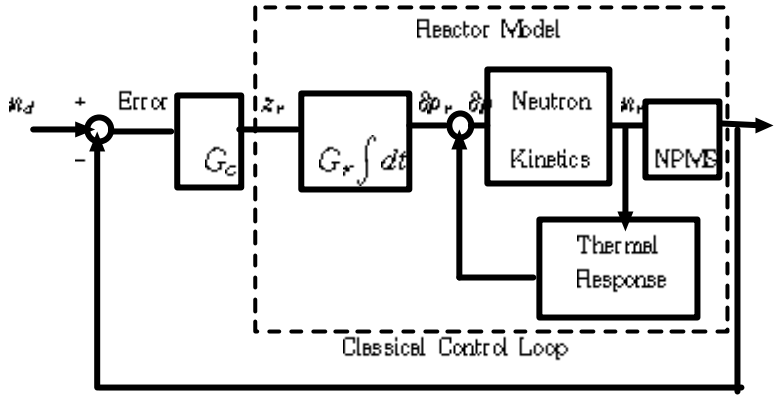

Figure 1. Reactor Model with Classical Output Feedback

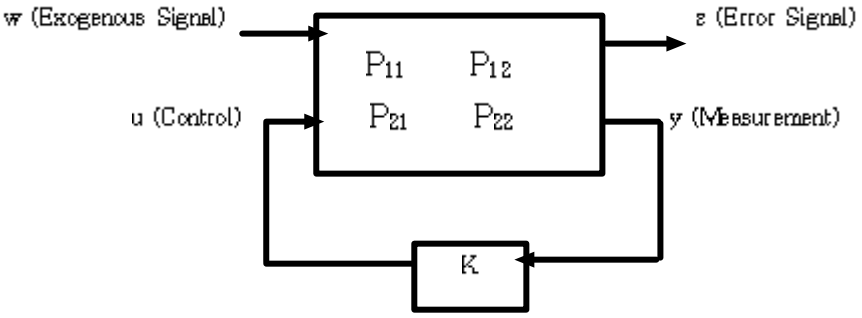

Figure 2. Block Diagram of Generalized Plant for H_∞ Controller Design

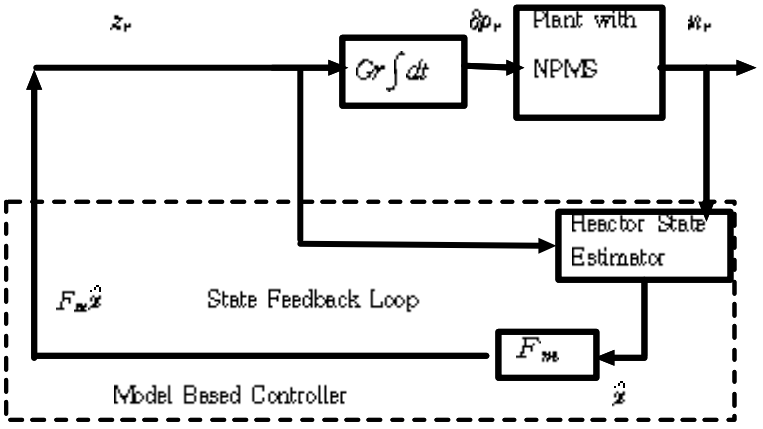

Figure 3. Model Based Controller with State Estimator and State Feedback

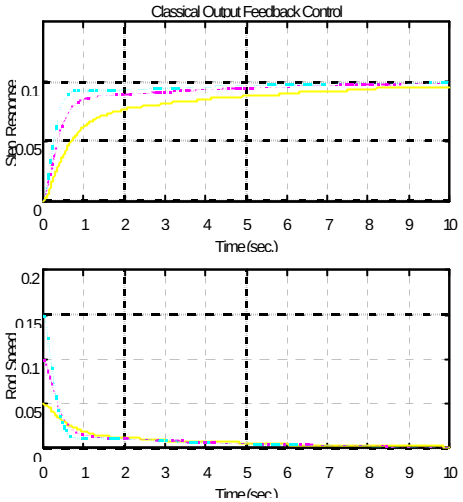

Fig.4 Step Response of Output Feedback Control
(Solid : Gc=0.5, Dashdot : Gc=1.0, Dotted : Gc=1.5)

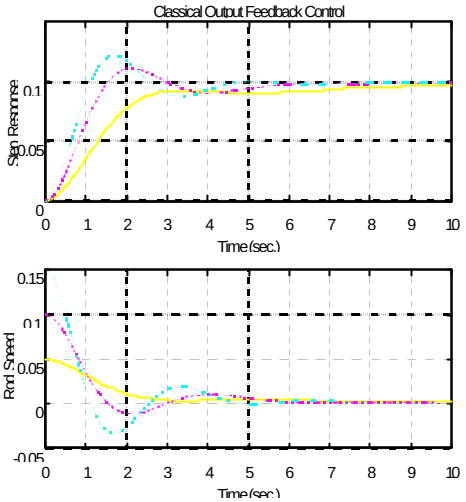

Fig.5 Step Response of Output Feedback Control
with Delayed Measurement
(Solid : Gc=0.5, Dashdot : Gc=1.0, Dotted : Gc=1.5)

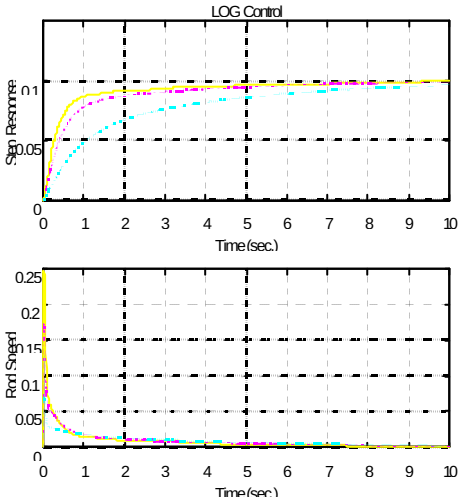

Fig.6 Step Response of LQG Control
(Solid : R=0.5, Dashdot : R=1.0, Dotted : R=5)

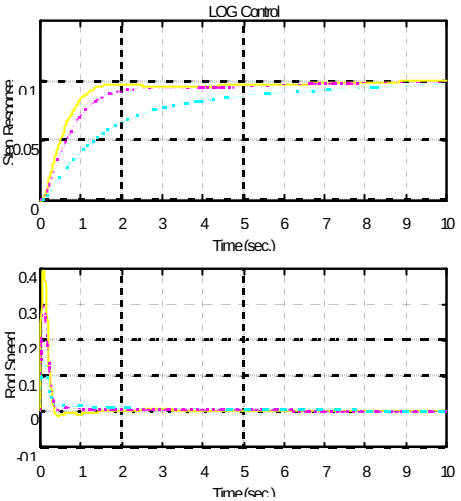

Fig.7 Step Response of LQG Control
with Delayed Measurement
(Solid : R=0.5, Dashdot : R=1.0, Dotted : R=5)

Case 1 : $W_T(s) = \frac{0.1s^2 + s}{325}$, $W_S(s) = \frac{1}{s + 0.0025}$.

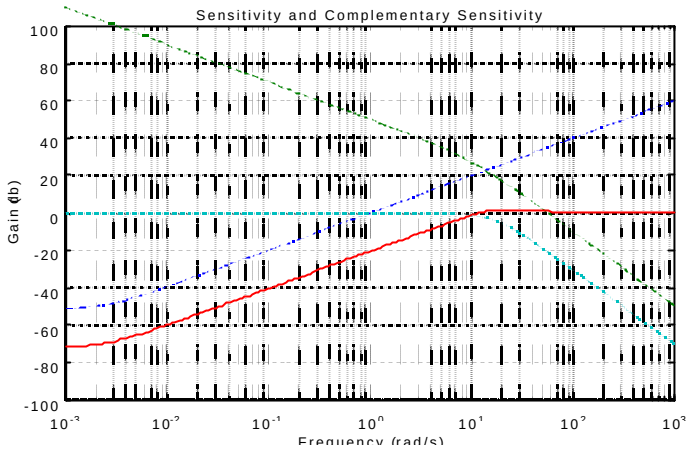

Case 2 : $W_T(s) = \frac{0.1s^2 + s}{5}$ $W_S(s) = \frac{1}{s + 0.0025}$

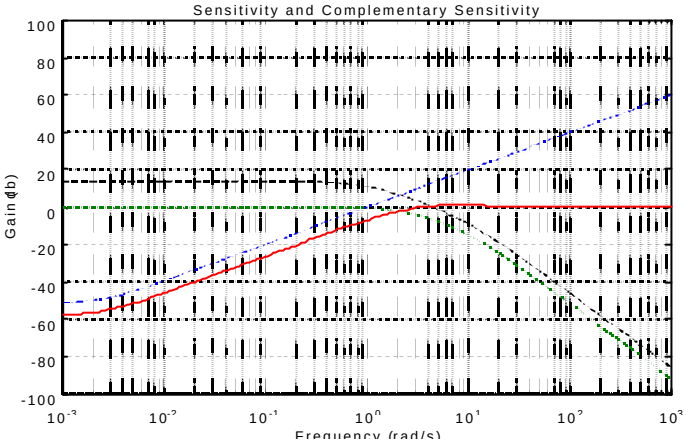

$\frac{1}{|W_T(s)|}$ $\frac{1}{|W_S(s)|}$ $S(s)$ $T(s)$

Figure 8. Gain of the Sensitivity and Complementary Sensitivity

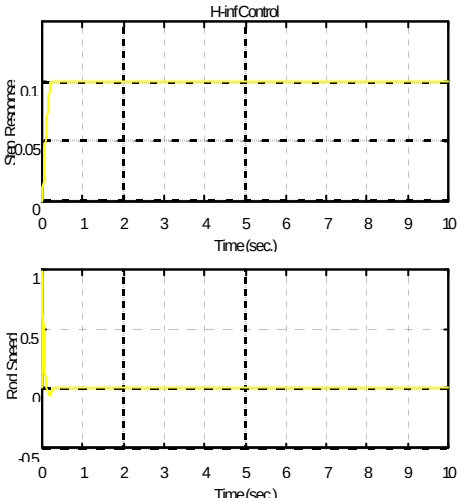

0,1) Fig.10 Step Response of H_∞ Control

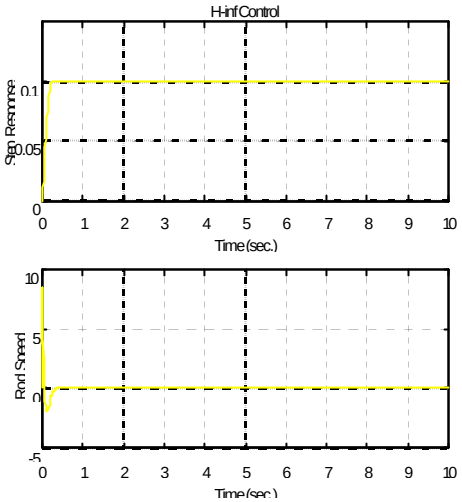

Fig. 9 Step Response of H_∞ Control (γ =

with Delayed Measurement (γ = 0,1)

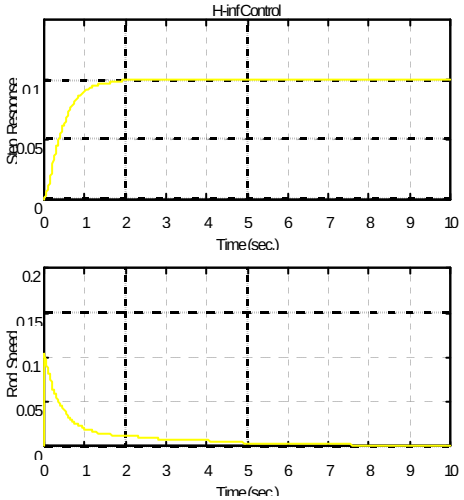

Fig.11 Step Response of H_∞ Control (γ = 0,5)

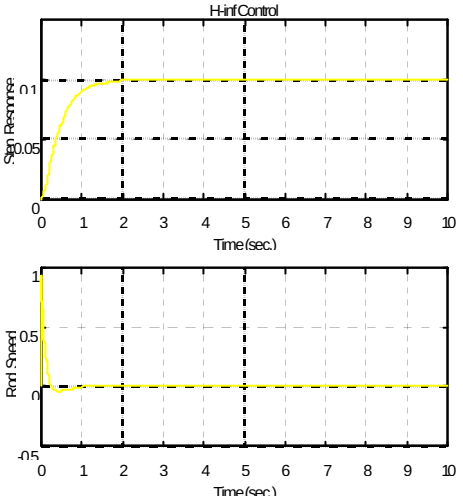

Fig.12 Step Response of H_∞ Control with Delayed Measurement (γ = 0,5)